ARMY RESEARCH LABORATORY

Study of Beta Radioisotopes Direct Energy Converters

by Y. Ngu and M. Litz

ARL-TR-4969   **September 2009**

Army Research Laboratory

Adelphi, MD 20783-1197

ARL-TR-4969   **September 2009**

Study of Beta Radioiostopes Direct Energy Converters

Y. Ngu and M. Litz
Sensors and Electron Devices Directorate, ARL

REPORT DOCUMENTATION PAGE

**Form Approved
OMB No. 0704-0188**

Public reporting burden for this collection of information is estimated to average 1 hour per response, including the time for reviewing instructions, searching existing data sources, gathering and maintaining the data needed, and completing and reviewing the collection information. Send comments regarding this burden estimate or any other aspect of this collection of information, including suggestions for reducing the burden, to Department of Defense, Washington Headquarters Services, Directorate for Information Operations and Reports (0704-0188), 1215 Jefferson Davis Highway, Suite 1204, Arlington, VA 22202-4302. Respondents should be aware that notwithstanding any other provision of law, no person shall be subject to any penalty for failing to comply with a collection of information if it does not display a currently valid OMB control number.
PLEASE DO NOT RETURN YOUR FORM TO THE ABOVE ADDRESS.

1. REPORT DATE (DD-MM-YYYY)	2. REPORT TYPE	3. DATES COVERED (From - To)
September 2009	Final	FY09

4. TITLE AND SUBTITLE	5a. CONTRACT NUMBER
Study of Beta Radioisotopes Direct Energy Converters	
	5b. GRANT NUMBER
	5c. PROGRAM ELEMENT NUMBER
6. AUTHOR(S)	5d. PROJECT NUMBER
Y. Ngu and M. Litz	
	5e. TASK NUMBER
	5f. WORK UNIT NUMBER

7. PERFORMING ORGANIZATION NAME(S) AND ADDRESS(ES)	8. PERFORMING ORGANIZATION REPORT NUMBER
U.S. Army Research Laboratory ATTN: RDRL-SED-E 2800 Powder Mill Road Adelphi, MD 20783-1197	ARL-TR-4969

9. SPONSORING/MONITORING AGENCY NAME(S) AND ADDRESS(ES)	10. SPONSOR/MONITOR'S ACRONYM(S)
	11. SPONSOR/MONITOR'S REPORT NUMBER(S)

12. DISTRIBUTION/AVAILABILITY STATEMENT

Approved for public release; distribution unlimited.

13. SUPPLEMENTARY NOTES

14. ABSTRACT

Energy stored in the nucleus of radioisotopes contains energy-densities five orders of magnitude higher than the energy-density of chemical bonds. The decay modes (and decay products) of these high-energy-density materials can then be matched to direct energy conversion materials for best efficiency. The choice of converter material, packaging geometry, thickness of material layer, and number of layers will necessarily depend on the specific radioisotope output product (alphas, betas, or gammas) and the energy of the particles (17 eV up to 5.5 MeV). Samples of silicon (Si) and silicon carbide (SiC) p-i-n diodes have been irradiated with betas from ^{90}Sr and ^{63}Ni. The voltage and current of the devices prior to irradiation were measured and compared to measurements made during periods of radiation. The sample diodes generate on the order of 10 pW in the presence of a 7.5 mCi source. This represents a direct-energy-conversion of beta-radiation to electrical power efficiency of ~7%.

15. SUBJECT TERMS

Direct energy conversion, isotope battery, beta-battery

16. SECURITY CLASSIFICATION OF:			17. LIMITATION OF ABSTRACT	18. NUMBER OF PAGES	19a. NAME OF RESPONSIBLE PERSON
a. REPORT	**b. ABSTRACT**	**c. THIS PAGE**	UU	22	M. Litz
Unclassified	Unclassified	Unclassified			**19b. TELEPHONE NUMBER** (Include area code) (301) 394-5556

Standard Form 298 (Rev. 8/98)
Prescribed by ANSI Std. Z39.18

Contents

List of Figures

List of Tables

1. Background

Awareness of power and energy priorities have been elevated in recent years because of the realization of the finite resources of oil, made clearer from our increasing rate of consumption. The solutions include both conservation and development and use of alternative energy sources. The military has much to gain from efficient platforms that reduce logistics burden, relieving the duty to protect the energy supply chain and thus saving lives in operational activities. Science and technology contributions in the form of ultra-light structural materials and alternative fuel auxiliary power capabilities are two areas that can have great impact. Alternative fuels include the use of fuel cells and rechargeable battery systems for electronic and Soldier power applications. Situational awareness (SA) technologies and unattended sensors that use renewable and rechargeable technologies are quickly helping to change the SA capabilities on the battlefield as well as in commercial activities.

Small-sensor technology is mission critical for future operational scenarios and depends on as-yet undeveloped micro-power sources. While many sensors are expendable for short-term applications, a host of sensors are required for longer-term applications. These sensors include environmental monitoring applications, embedded sensors for materials and structural integrity, and place-and-forget sensors to monitor personnel movement in caves and tunnels. The power levels associated with unattended sensors coincide with those of typical energy harvesting applications. Energy conversion and storage technologies are fundamental to the harvesting of energy from the local environment. Energy harvesting techniques can have particular impact in micro-power applications (1 nW to 100 mW) and Soldier power (1 W to 100 kW) regimes.

The needs of the Army are not stagnant. At this time, the real-time demands to adapt to the environment, increase operational pace, and operate within logistical limitations have never been greater. Nuclear batteries can have a small but significant impact as a power sources for long-lived sensors (*1–3*). Consider embedded sensors for bridges and foundations of large buildings. These sensors can provide information about the structural integrity (*4–6*). Unattended sensors for temperature measurement in the oceans would need no maintenance during an increased operational lifetime. Unique opportunities are waiting for sensors and radio frequency identification (RFID) tags that benefit from keep-alive power lasting decades.

Chemical power sources can store the total energy required, but electrical leakage and deterioration of the batteries keeps them from delivering the power over a decade. Nuclear batteries offer a unique power-source to fill the niche. Even though the energy-density of nuclear isotopes is six orders of magnitude greater than that possible in chemical bonds, the stigma associated with nuclear materials will require careful design and thoughtful application. Sensors embedded in structures, providing information useful to monitor structural integrity (i.e., bridges, helicopter blades), may be just the application to overcome these difficulties.

Eliminating the need to maintain power for small sensors can save lives, especially if the sensors are in the middle of the battlefield. It can also be operationally important for sensors to remain covert. These hidden sensors must remain powered for long periods to maintain the element of surprise. Costly maintenance can be avoided when the sensors are not accessible (i.e., at the bottom of tunnels, under water, within walls). The crossover point for deciding on the use of small isotope powered batteries versus chemical batteries depends primarily on the system power requirements and the length of time required to operate. As an example of a representative sized system, several small sensors in the inventory, using AA and AAA batteries, require power levels of 90 to 9000 mW. The maintenance rate for these useful sensors unfortunately puts Soldiers in harm's way on a daily basis, making the sensors unusable in many scenarios.

A sensor requiring 100 mW will drain a single AAA battery in less than one day. The power drain is compared to battery capacity in figure 1. If 1 W is required by the sensor/load, then the 1 kg BA5590 will last less than 1 week. The niche for isotope batteries is in situations where sensors with relatively low power consumption can be combined with the large amounts of energy stored, permitting operational power sources that minimize maintenance schedules, saving lives and maintaining covert operations and the element of surprise. Long-lived sensors (>10 years) benefit from isotope-based batteries.
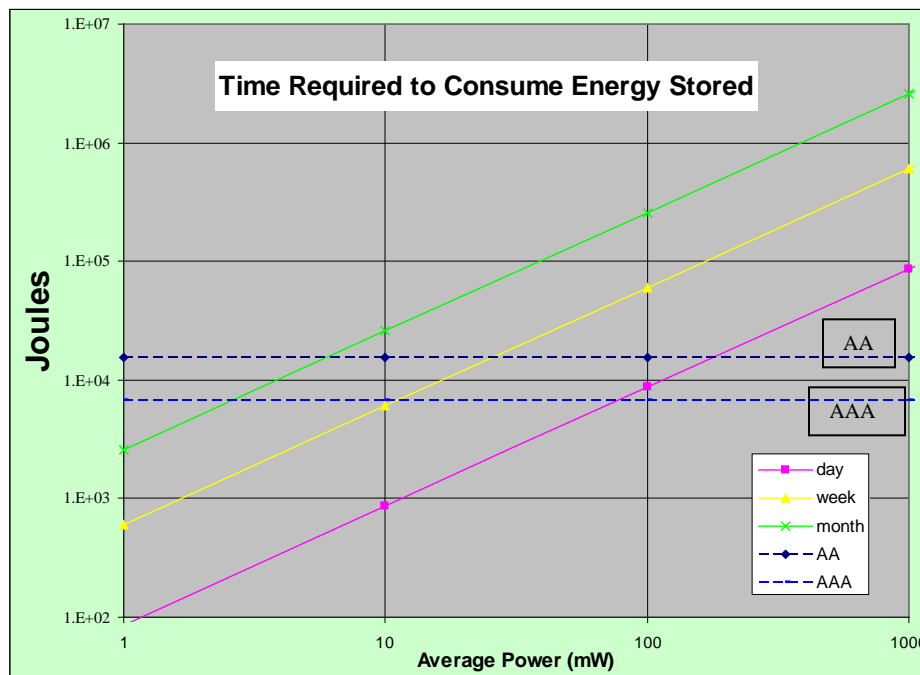
Figure 1. A 100 mW sensor uses one AAA battery per day. This energy demand creates large logistics requirements that are difficult to support.

The energy stored in batteries is insufficient to last for the longer periods of time that are relevant to military operations. A 10-mW load will use the energy stored in an AA battery in less than a month. A 100-mW load will use the energy stored in a BB3590 in less than 6 months. If 1 W is required by the sensor/load, then the 1 kg BB5590 will last less than 1 week. Figure 2 shows the energy stored in several commercial and military style batteries in common use.
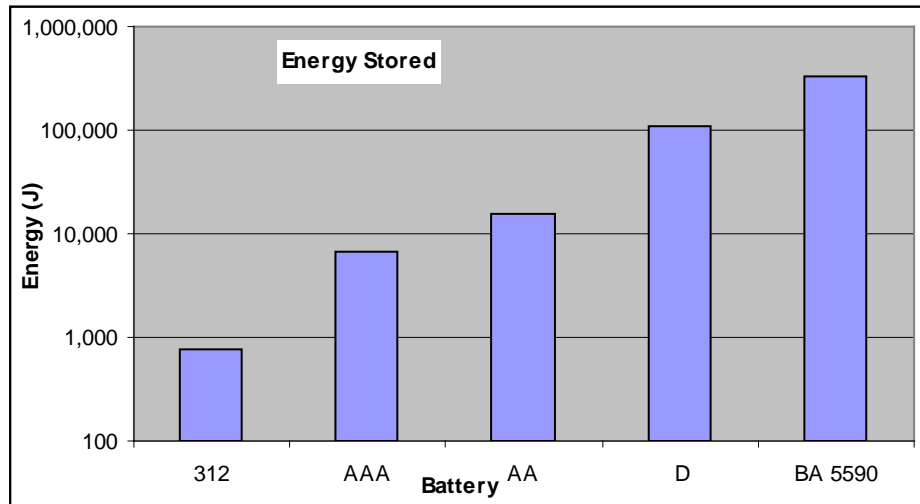
Figure 2. Energy stored in several commercial and military style batteries in common use.

We have examined the energy conversion capability of multiple semiconductor-based direct energy conversion devices. In this report, we analyze the structure of single diodes as it pertains to its conversion efficiency and investigate diode architectures to enhance the overall delivered energy by stacking individual devices in parallel. This report is structured as follows: section 2 presents the various devices used and their mode of operation, section 3 presents the measurement setup, section 4 offers measurement results and a discussion of our observations, and section 5 provides closing remarks.

2. Devices

Semiconductor-based radioisotope power converters use the energy generated by the decay of radioisotopes to create a power source. A battery of this type is composed of two main parts: (1) a radioisotope source of energy and (2) an energy converter (diode) that changes the radiation output of the radioisotope energy source into some form of usable electrical energy.

The devices used for energy conversion were silicon carbide (SiC) p-i-n diodes. These diodes differed by the thickness of their i-layer and the size of their active area. The names used to describe the cells as well as their i-layer size and die size are tabulated in table 1.

Table 1. Device description.

Diode #	1	2	3	13	14	Q1	Q2	Q3	Q4	Q5	Q6	Q7
i-layer (μm)	60	60	80	110	110	50	42	35	30	20	10	5
Die size (cm)	0.5	0.5	0.5	0.5	0.5	1	1	1	1	1	1	1

Diode #	S11	S12	S21	S22	E11	E12	E41	E42	E62	E72	E81	E82
i-layer (μm)	60	60	60	60	60	60	60	60	60	60	60	60
Die size (cm)	0.5	0.5	0.5	0.5	0.5	0.5	0.5	0.5	0.5	0.5	0.5	0.5

The devices from table 1 were electrically accessed via three type of connection. The devices having only numeric numbers (i.e., 1, 2, 3 …) were electrically accessed via leads affixed to the metal seed layer of the front (n-layer) and back (p-layer). The diodes were mounted at the center of a holder such that the backside of the diode was mounted via conducting epoxy to a conducting holder and the front side of the diode had small conducting wires soldered to it and pulled-out to form a lead, as illustrated in figure 3 (left).

The devices having alpha-numeric number with a single digit (i.e., Q1−Q7) were electrically accessed with a test fixture. These devices were dies and were not permanently attached to the holder. Contact was made to the front side of the die (n-layer) via a probe-like contact; while, the backside (p-layer) of the die sat on a copper line given electrical contact to the backside. This setup is shown in figure 3 (right).
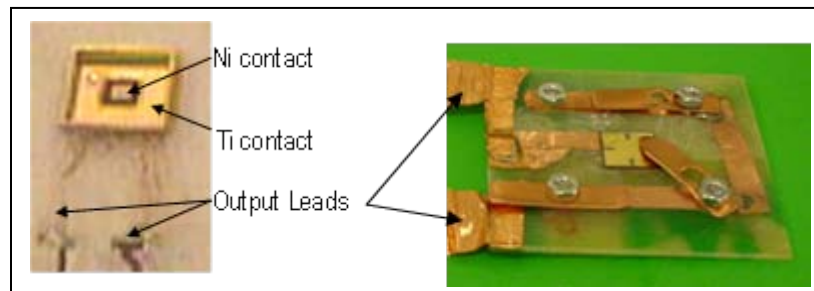
Figure 3. (Left) Diode layout and contact for diode# 1−14 (left) and diode# Q1−Q7 (right).

The devices having alpha-numeric number with two digits (i.e., S11−E82) were electrically accessed via copper strips affixed with conducting epoxy directly to n-layers and p-layers. All these devices were pairs of diodes mounted back-to-back, as shown in figure 4. A copper strip was sandwiched between the back-to-back diodes to enable contact to each diode's n-layer, referred to as the negative terminal (see figure 4 (a)). For devices with numbers starting with E, each p-layer of the diode pair had a copper strip epoxy to it (see figure 4 (a)); whereas, the devices with numbers starting with S only had one diode with a copper strip epoxy to it while the other p-layer was left bare (see figure 4 (b)). The copper strips affixed to the n-layers are referred to as the positive leads. There was a 3-mm hole in the copper strip at the center of the diode to enable our radioisotope source to be in close contact to the p-layers (see figure 4 (c) and (d)).
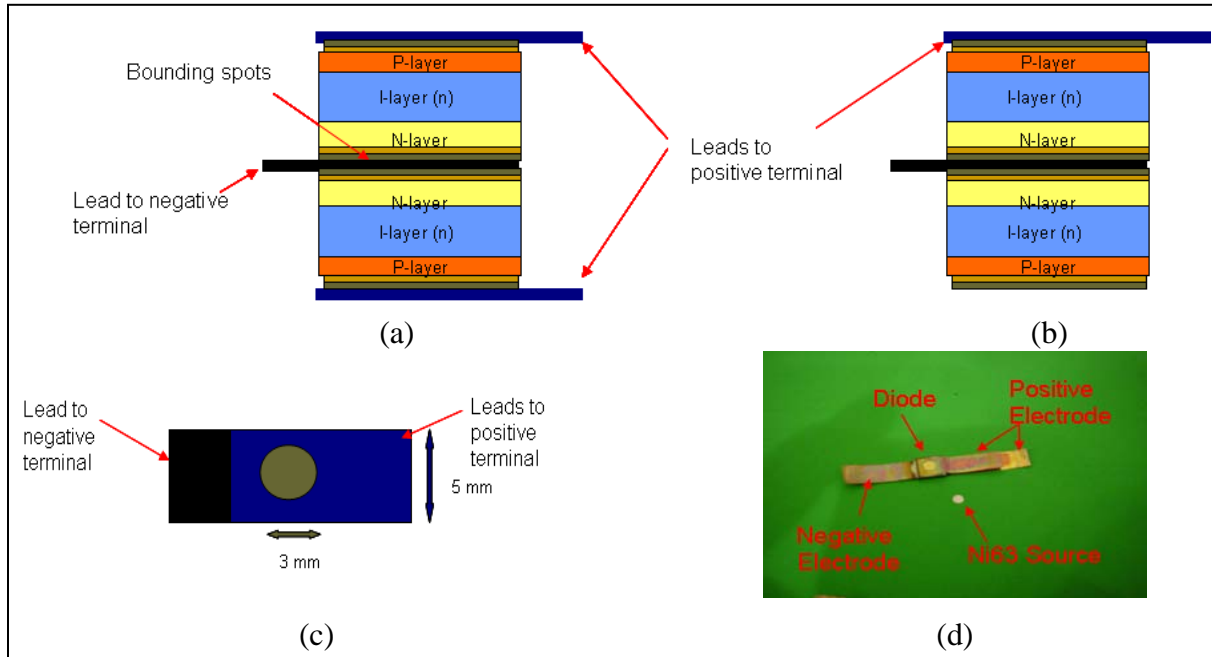
Figure 4. SiC p-i-n diode pairs: (a) diode layout with three leads (diodes numbered Exx); (b) diode layout with two leads (diodes numbered Sxx); (c) top view of the diode pairs; and (d) picture of the three-lead diode pair.

3. Measurement Setup

The energetic particles emitted during the decay of the radioisotopes create a multitude of electron-hole pairs within the semiconductor (*7*). Once the carriers are generated, positive charges flow into the semiconductor and lead to a generated current Ig, which is equivalent to a short circuit current (*Isc*). The displaced carriers effectively forward bias the p-layer, as seen in figure 5 (a), hence creating a voltage potential across the device. The forward bias junction yields a current (*Id*) through the junction that is opposite to the generated current. In the presence of very small load (short), $Isc = Id$, while the output voltage with very high load (open) is Voc, the open circuit voltage. When a load is connected to the diode's output terminals, as in figure 4 (b), the current due to the forward bias junction is split between the current into load (*Iout*) and *Id* such that $Ig = Id + Iout$.
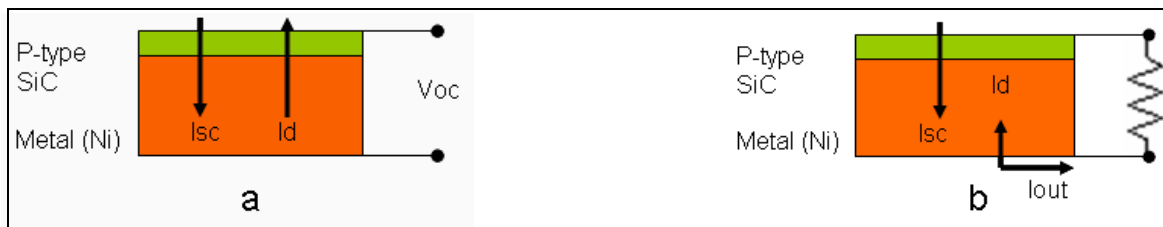
Figure 5. Current flow under (a) open circuit and (b) load conditions.

5

In order to characterize the conversion effectiveness of our diodes, the current through the diode, as well as the potential across it, needed to be monitored. The conventional approach is to perform current versus voltage (I-V) plots, where the voltage across the diodes is swept and the current across the diode is recorded. This procedure is then done with no radioisotope ("dark" or "baseline" measurement) and in presence of the radioisotope ("radiation"). In the presence of radiation, the potential at zero current flow corresponds to open circuit voltage (Voc) while the current at zero potential corresponds to short circuit current (Isc). It is expected that the baseline and radiation I-V curve would follow the same trend as a photovoltaic cell. The I-V curve of a conventional photovoltaic cell is shown in figure 6.
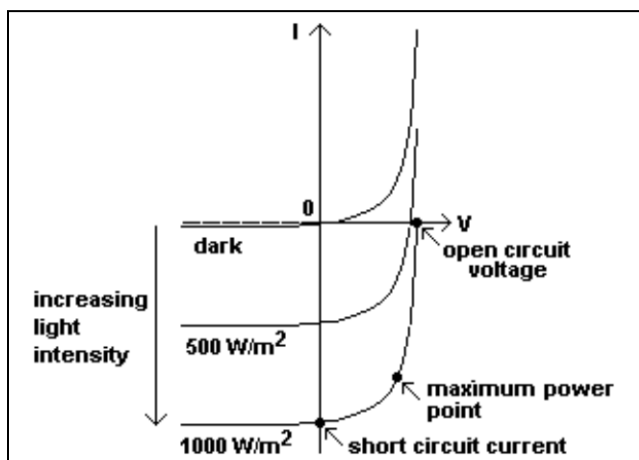
Figure 6. I-V curves of a conventional photovoltaic cell
with and without light.

Electrical measurements of the diode I-V curve were done with parameter analyzers (HP5155C and HP5145). The samples were radiated with ^{90}Sr and ^{63}Ni. The ^{90}Sr radiation measurements were conducted at the Naval Surface Weapons Center-Carderock (NSWC), MD, using a J. L. Shepherd 10 mCi ^{90}Sr cabinet. The ^{63}Ni measurements were conducted with a small (2 mm diameter and 50 µm thick) individual coating source sputtered on a thin metal layer. These sources can be paired, as illustrated in figure 7, such that their metal layers are in contact, which enables the diodes to be stacked. Prior to radiation, baseline I-V curves were recorded then a radiation I-V curve was recorded during radiation. The I-V curve was conducted between –2 V and 2 V by 10 mV increments and long integration (each data point corresponds to the average of 16 samples). The parameter analyzer was connected to the diodes via alligator clips.
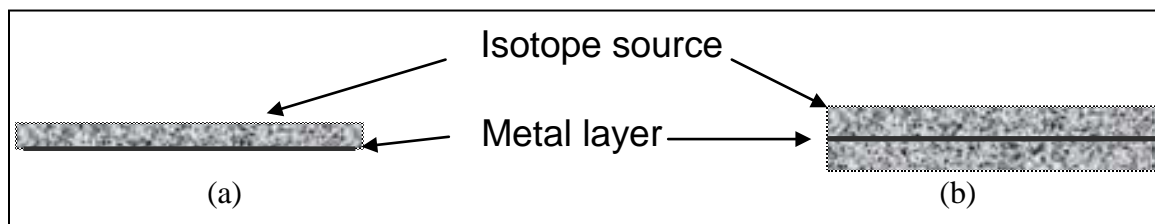
Figure 7. ^{63}Ni radioisotope sources: (a) single source and (b) source pair.

In order to increase the overall output current of our direct-energy-conversion (DEC) cell we laid out diodes in parallel. The parallel structure is assembled by stacking the diodes in separated ^{63}Ni source pairs. In this arrangement, the copper leads to the p-layers were all connected together with copper tapes to make a single positive leads. The same was done with the leads to the n-layers to make the negative lead of the stacked structure. A schematic of the stacked cell is shown in figure 8.
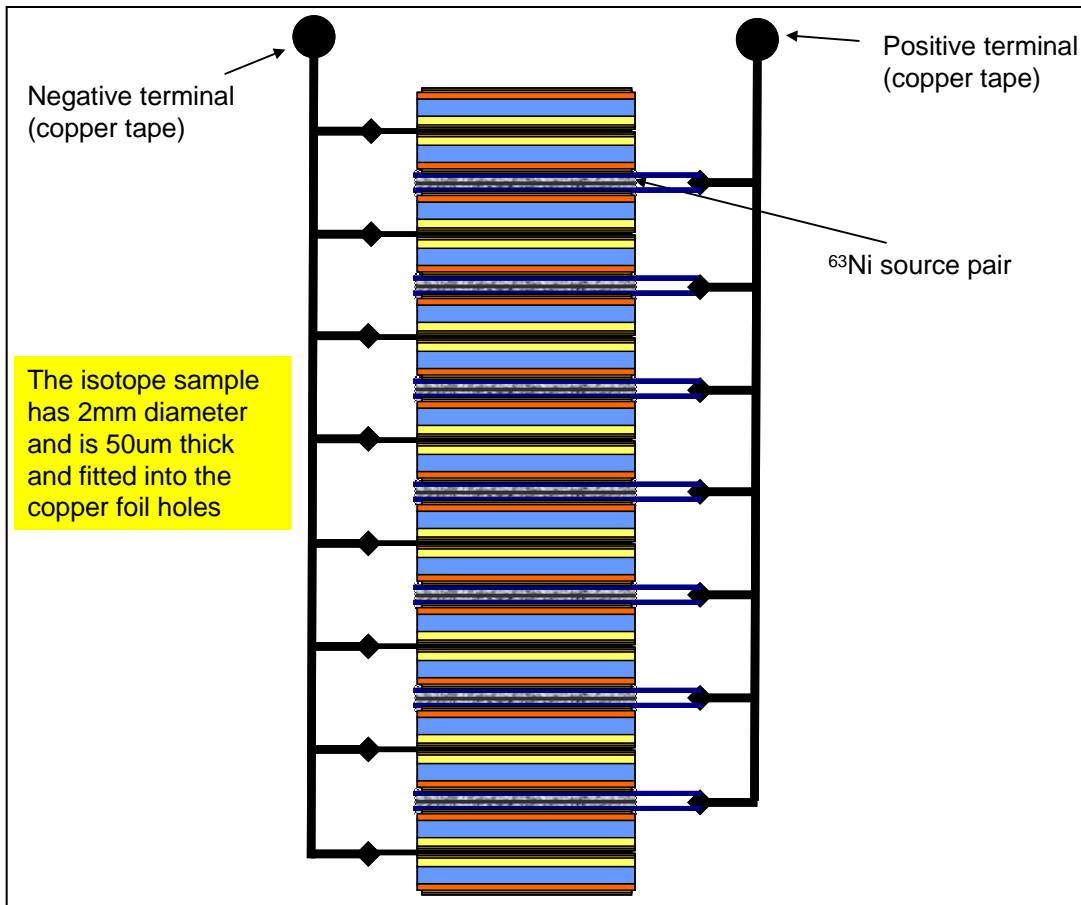
Figure 8. Eight stacked diode pairs with 14 sources (7 pairs).

4.   Results and Discussion

Before performing any radiation measurements, a baseline measurement was conducted for all diodes. The baseline measurement is, in effect, a way to test that the cell has proper diode behavior. The baseline measurement for the Qynergy diodes is shown in figure 9. In the plot, it can be seen that the diodes Q3, Q4, and Q7 do not operate normally—the turn-on point of the diodes is at zero potential. No further radiation evaluations were conducted on the diodes that were deemed dysfunctional (i.e., Q3, Q4, and Q7). The same measurements were conducted on the rest of the diodes and diodes 2, E31, E32, E61, and E71 were also excluded.
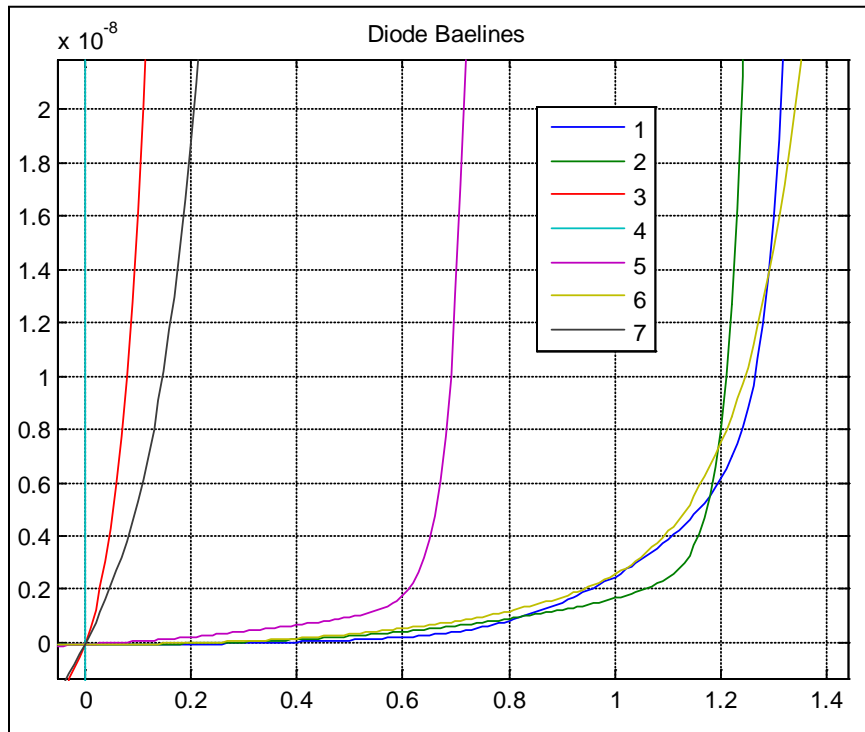
Figure 9. Baseline I-V curve of Qynergy diodes (diodes Q1–Q7).

Once the diodes were screened for proper operation, the radiation measurement was conducted by applying the radiation and recording the I-V curve. Figure 10 shows I-V curves from 0 to 1.2 V for various diodes. The radiation curves are lower than their baseline counterparts, as expected. The baseline current at zero potential represents the diodes leakage current; hence, the generated current is the difference between the baseline current and the radiation current at zero potential. As seen in figure 10 (c), the generated current was found to be as high as 30 pA or as low as 2 pA in the case of figure 10 (a) and (b).
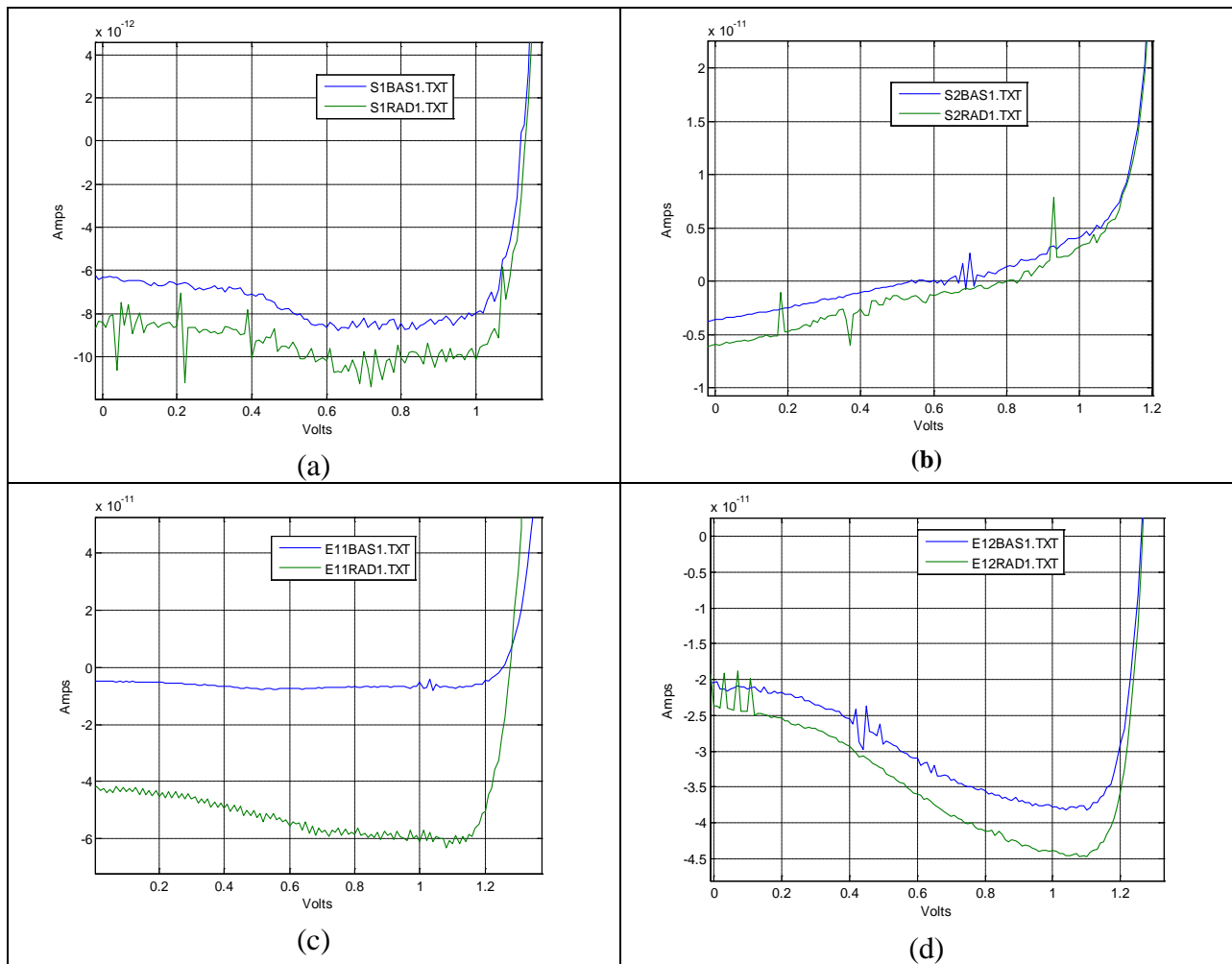
Figure 10. Baseline and ^{63}Ni radiation I-V curve: (a) diode S11; (b) diode S21; (c) diode E11, and (d) diode E12.

The generated current from a single diode was determined to be quite low (sometime as low as 2 pA), so we decided to increase the effective generated current by placing the cells in parallel. We tried placing two then four diodes in parallel. Figure 11 presents the I-V curves obtained from radiation measurement of the diodes in parallel. In figure 11 (a), D1 and D2 refer to the diode S11 and S21, respectively, while D1–2 refers to the parallel combination of the two diodes (S11 and S21). The generated current is effectively equivalent to the sum of the individual radiation currents of each diode; however, this was not the case once four diodes were placed in parallel, as can be observed in figure 11 (b), referred to as P4. In both cases, the I-V curve of the parallel structure was not the sum of the individual diodes over the entire curve. This behavior is potentially due to internal mismatches between diodes. The leakage current and turn-on voltage of each diode was different and this could lead to one diode acting as a load on another. When

the diode is off (current is negative), the current from one diode flows through another diode instead of the external loop through the parameter analyzer; hence, the recorded parallel current is less than the sum of each diode.
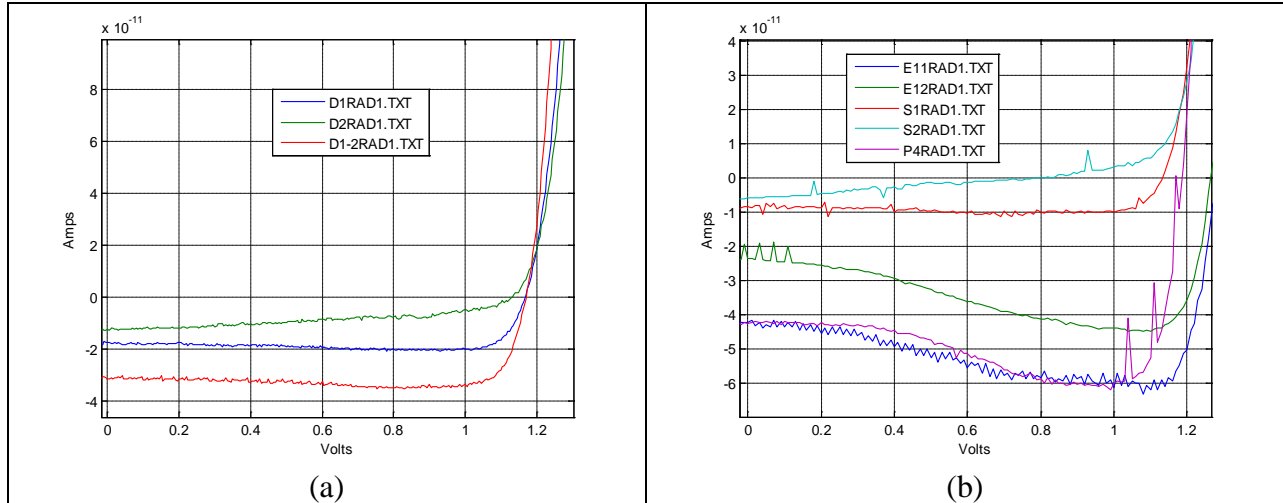
Figure 11. ^{63}Ni radiation I-V curve: (a) diodes S11 and S21 as single diode and in parallel (D1-2) and (b) diodes E11, E12, S11, and S21 as single diode and in parallel (P4).

To maximize the current output, we put eight diode pairs in parallel. This setup used 14 active diodes and ^{63}Ni sources. Since the output current obtained from the other parallel combinations (two and four diodes) did not yield a linear increase in current over the entire I-V curve, we decided to look at the generated current out of this stacked structure over time at zero bias. We grounded the n-layer leads and applied 0 V at the p-layer leads and recorded the current through the diodes over a 40-s period. The generated current from the eight stacked diode pairs is shown in figure 12. The background current identifies the current recorded in the lab with no ^{63}Ni source. The stacked diodes generated approximately 2 pA. The generated current was quite similar to that obtained from the previously recorded single diode measurements (see figure 10). Again, this might be due to the diodes loading each other as well as to an odd behavior observed in some of the I-V curves.
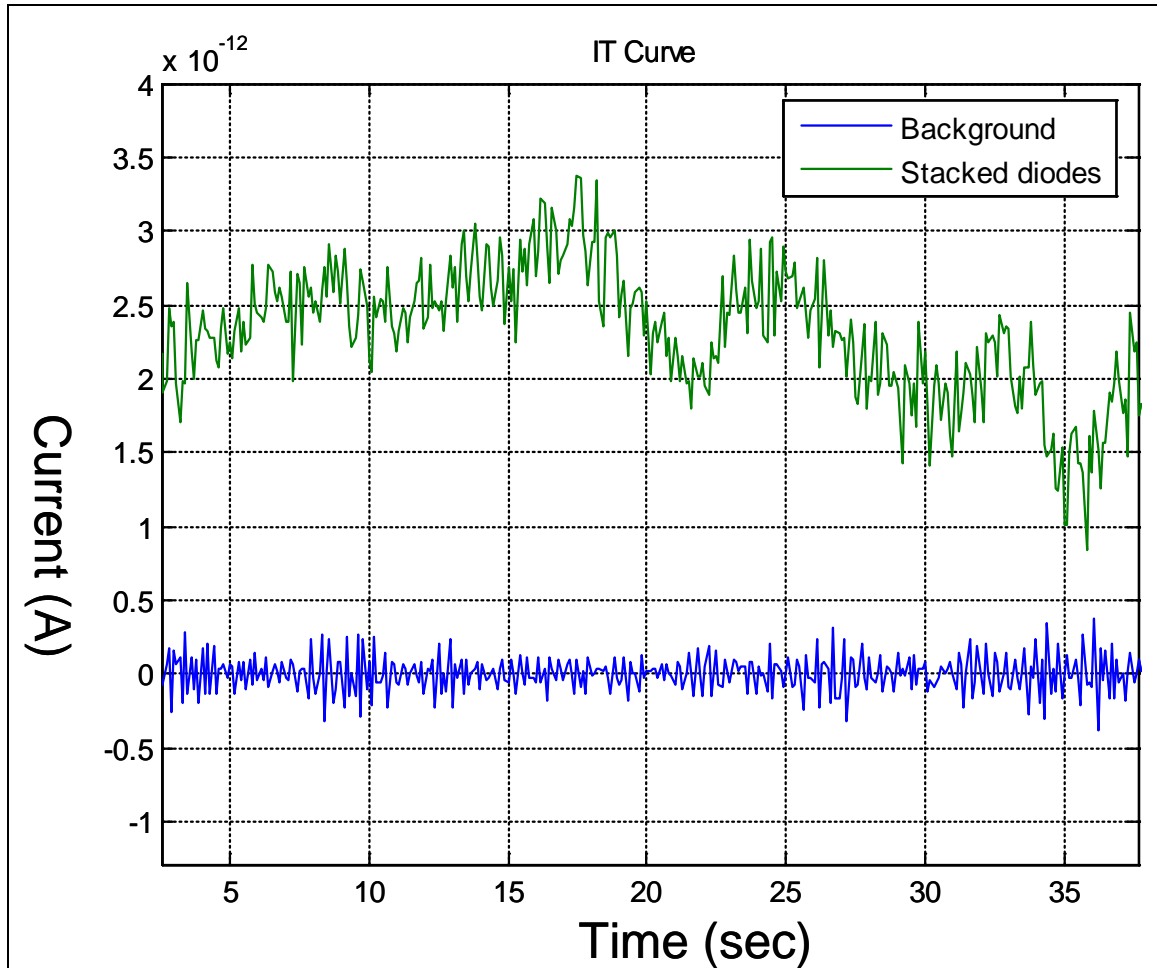
Figure 12. ^{63}Ni radiation time vs. current with no biasing of stacked structure. The background line represents lab noise and the stacked diodes line is the radiation measurement.

The I-V curves of some of our diodes followed the unexpected example trained shown in figure 13, where the radiation generated I-V curve is higher than the baseline curve. This behavior could be explained by the idea that the generated current might be flowing in the opposite direction to what is commonly expected. Another explanation could be that we could have been measuring very close to the sensitivity level of the tool (we were in the pico range). The I-V curve recorded in figures 10 (a) and 13 were conducted on the same diode on two separate days. Each behavior was observed more than once in this and other diodes.
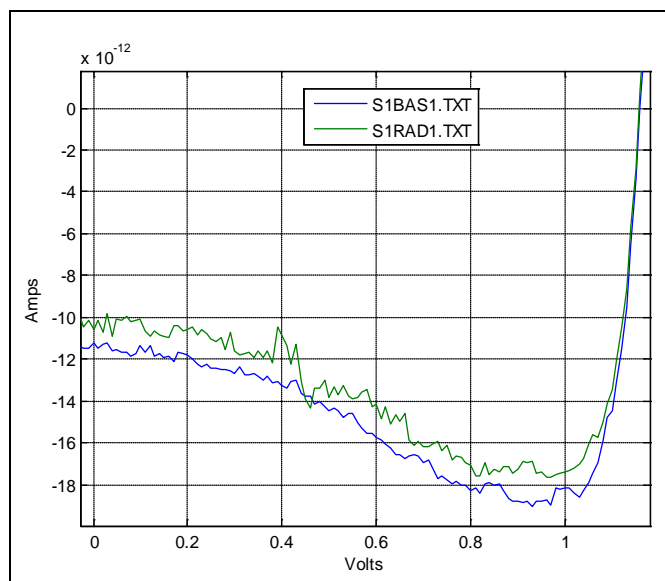
Figure 13. ^{63}Ni radiation, showing unusual radiation data from a properly functioning diode (diode S11).

5. Conclusions

Semiconductor-based radioisotope power converters use the energy generated by the decay of radioisotopes to directly create a current/power source. Thermal energy conversion is used for reactors, but that is not practical for compact packaging. In this report, we have characterized SiC p-i-n diodes for energy conversion efficiency. Power output was measured using an I-V curve tracer. These diodes differed by the thickness of their i-layer and the size of their active area. In order to characterize the conversion effectiveness of our diodes, the current through the diodes was monitored by performing I-V plots while sweeping the voltage across the diodes. The generated current varied as high as 30 pA and as low as 2 pA for a single diode. Stacking the diodes in parallel did not lead to a linear increase in generated current when using up to 14 diodes. Three stacking approaches (2, 4, and 14 diodes in parallel) were compared. This result was most likely due to a diode mismatch in the structure, which decreased with the number of diodes in the stack.

The overall small current and voltage obtained in our preliminary work was due to the large size of the depletion region of the diode used (~100 to 500 µm). The efficiency of the diodes can be improved by optimizing the diodes (p-i-n layer thicknesses) for our specific application and choice of isotope (*7*). In the future, designs for devices will permit increased generated current and open circuit voltage by matching the i-layer thickness with the energy of the electron emitted from the isotope decay. Depending on the isotope used and the length of time to be operated, SiC p-i-n diodes could be substituted in place of Si p-i-n diodes for longer operation, because SiC is more resistant to radiation damage. The isotope used in these experiments was Ni^{63},

which emits β particles with 17.4 keV energy. This energy can be absorbed by a >40-µm layer of Si without creating any significant defect in the semiconductor. The Ni^{63} used in these experiments were 2-mm circular foils and the SiC diodes used for the preliminary work were 5 mm × 5 mm SiC square diodes. In order to increase the rate of emission (and therefore the generated current), we need to increase the activity of the radioactive foils. Ni^{63} foils are commonly used for detection of explosives in Homeland Defense initiatives and as a power source for remote instrumentation.

Alternative isotopes with the long half-lives and low-energy beta emission exist. Half-lives greater than 50 years are useful, because then batteries could be designed to last the lifetime of the infrastructure. Sensors buried inside buildings that operate the lifetime of the structures would require no maintenance. The other useful characteristic of a beta source is that the beta (electron) emitted has a low energy reducing potential for radiation damage to the semiconductor converter. Ni^{63} has a 101-year half-life and a 17 keV average beta energy. Three other isotopes with similar parameters are (1) Tb^{157} with a 99-year half-life and 63 keV average beta energy; (2) Sm^{151} with a 90-year half-life and 76 keV average beta energy; and (3) Pt^{193} with a 50-year half life and 56 keV average beta energy.

6. References

1. Blanchard, J. P. Stretching the Boundaries of Nuclear Technology. *The Bridge* **2002**, *32* (4), 29–34.

2. Ahearne, J. F. The Future of Nuclear Energy, editorial. *The Bridge* **2001**, *31* (3), 3.

3. Bugliarello, G. Our Energy Future, editorial. *The Bridge*, *32* (2), 3–4.

4. Lal, A.; Blanchard, J. The Daintiest Dynamos. *IEEE Spectrum* **Sept. 2004**, 36–41.

5. Lal, A.; Blanchard, J. By Harvesting Energy from Radioactive Specks, Nuclear Micrbatteries Could Power Tomorrow's Microelectromechanical Marvels-And May Be Your Cellphone Too. *IEEE Spectrum*, **September 2004**, 36–41.

6. Litz, M.; et al. On-Demand High Energy Density Materials, *Proceedings of 3rd IECEC*, San Francisco, CA.

7. Guo, H.; Lal, A. Nanopower Betavoltaic Microbatteries. *The 12th International Conference on Solid State Sensors, Actuators and Microsystems*, Boston, 8–12 June 2003.

8. Guo, H.; Yang, H.; Zhang, Y. Betavoltaic Microbatteries Using Porous Silicon, *MEMS 2007*, Kobe, Japan, 21–25 January 2007.

List of Symbols, Abbreviations, and Acronyms

DEC   direct energy conversion

I-V   current versus voltage

NSWC   Naval Surface Warfare Center

RFID   radio frequency identification

SA   situational awareness

Si   silicon

SiC   silicon carbide

No. of Copies	Organization
1 ELECT	ADMNSTR DEFNS TECHL INFO CTR ATTN DTIC OCP 8725 JOHN J KINGMAN RD STE 0944 FT BELVOIR VA 22060-6218
1	DARPA ATTN IXO S WELBY 3701 N FAIRFAX DR ARLINGTON VA 22203-1714
1 CD	OFC OF THE SECY OF DEFNS ATTN ODDRE (R&AT) THE PENTAGON WASHINGTON DC 20301-3080

1	US ARMY RSRCH DEV AND ENGRG
	  CMND
	ARMAMENT RSRCH DEV AND ENGRG
	  CTR
	ARMAMENT ENGRG AND TECHNLGY
	  CTR
	ATTN AMSRD AAR AEF T J MATTS
	BLDG 305
	ABERDEEN PROVING GROUND MD
	  21005-5001

1	PM TIMS, PROFILER (MMS-P) AN/TMQ-52 ATTN B GRIFFIES BUILDING 563 FT MONMOUTH NJ 07703
2	US ARMY ARDEC ATTN AMSRD AAR AEM L S GILMAN, BLDG 65S ATTN AMSRD AAR MEE W S SINGH BLDG 3022 PICATINNY ARSENAL NJ 07806-5000

No. of Copies	Organization
1	US ARMY INFO SYS ENGRG CMND ATTN AMSEL IE TD A RIVERA FT HUACHUCA AZ 85613-5300
1	COMMANDER US ARMY RDECOM ATTN AMSRD AMR W C MCCORKLE 5400 FOWLER RD REDSTONE ARSENAL AL 35898-5000
1	US GOVERNMENT PRINT OFF DEPOSITORY RECEIVING SECTION ATTN MAIL STOP IDAD J TATE 732 NORTH CAPITOL ST NW WASHINGTON DC 20402
1	US ARMY RSRCH LAB ATTN RDRL CIM G T LANDFRIED BLDG 4600 ABERDEEN PROVING GROUND MD 21005-5066

16 HCS
2 CDS
	US ARMY RSRCH LAB
	ATTN IMNE ALC HRR MAIL &
	  RECORDS MGMT
	ATTN RDRL CIM L TECHL LIB
	ATTN RDRL CIM P TECHL PUB
	ATTN RDRL SED E G MERKEL
	ATTN RDRL SED E J TATUM
	ATTN RDRL SED E M LITZ
	  (12 COPIES)
	ATTN RDRL SER M E ADLER
	ADELPHI MD 20783-1197

TOTAL: 29 (25 HCS, 1 CD, 3 ELECT)